Supplementary Information (SI) for Materials Chemistry Frontiers.
This journal is © the Partner Organisations 2024

Supplementary Information

Engineering a Versatile Nanoscale COF-Based Multienzyme Loading Strategy to Enhance Cancer Therapy

Wen-Xiu Ren, †[a] Qing-Yun Huang, †[a] Jie Feng, [a]* Yue-Lu Tian, [a] Ya-Ni Wu, [a] Seeram Ramakrishna,[b] Yu-Bin Dong [a]

[a] College of Chemistry, Chemical Engineering and Materials Science, Collaborative Innovation Center of Functionalized Probes for Chemical Imaging in Universities of Shandong, Key Laboratory of Molecular and Nano Probes, Ministry of Education Shandong Normal University, Jinan 250014, People's Republic of China.

[b] Centre for Nanotechnology and Sustainability, Department of Mechanical Engineering, National University of Singapore, 117574 Singapore, Singapore.

* Correspondence author. E-mail: jiefeng@sdnu.edu.cn

‡ These authors contributed equally to this work.

Experimental section

1. Materials and instruments

Materials: All reagents are analytically pure and used directly without further purification. Glacial acetic acid, Zinc nitrate hexahydrate, Potassium permanganate ($KMnO_4$), N, N-Dimethylformamide (DMF) and ethanol were purchased from Sinopharm Chemical Reagent Co., Ltd., 1,3,5-tris(4-aminophenyl)benzene, 2,5-dimethoxyterephthalaldehyde and were all purchased from Jilin Yanshen Technology Co., Ltd., 2-methylimidazole (2-MIM), Trypsin, Lipase, Urease, Pancreatin, glucose oxidase (GOx), (4,5-dimethyl-2-thiazolyl)-2,5-diphenyl-2-H-tetrazolium bromide (MTT), Methylene blue (MB), hydrogen peroxide (H_2O_2), were purchased from Sigma-Aldrich (Shanghai) Trading Co. Ltd., Ribonuclease A, Lysozyme, horseradish peroxidase (HRP), Rhodamine B, Pyrogallic, Fluorescein5 (6)-isothiocyanate (FITC), Dimethyl sulfoxide (DMSO) and N-Ethylmaleimide(NEM) were purchased from Shanghai Macklin Biochemical Co., Ltd., 3,3',5,5'-Tetramethylbenzidine (TMB) and 5,5'-Dithiobis-(2-nitrobenzoic acid)(DTNB) were purchased from was Aladdin Reagent (Shanghai) Co., Ltd., Hydrogen Peroxide Assay Kit, Lyso-Tracker Red, Mito-Tracker Red CMXRos, Hoechst 33342, glutathione(GSH), ROS Kit (DCFH-DA), pH Fluorescent Probe (BCECF AM), Mitochondrial Membrane Potential Test Kit (JC-1) and ATP Assay Kit were obtained from Beyotime Biotechnology Co., Ltd. Dulbecco's phosphatebuffered saline (DPBS), and fetal bovine serum (FBS) were purchased from Biological Industries USA. RPMI Medium Modified (1640) was purchased from HyClone Laboratories, Inc. 4% formaldehyde universal tissue fixative was purchased from Biosharp Co., Ltd. HL-7702 (normal human liver cells) and mouse breast cancer (4T1) cells were purchased from the Procell Life Science & Technology Co., Ltd.

Instrument: Fourier transform infrared (FT-IR) spectra were obtained in the 4000–400 cm^{-1} range using a Thermo Scientific Nicolet iS50 FT-IR Spectrometer equipped with diamond attenuated total reflection (ATR) module. Each spectrum was the average of 16 scans. Ultraviolet–visible (UV-vis) absorption spectra were recorded on a Shimadzu UV-2700 Double Beam UV-vis Spectrophotometer. Scanning electron microscopy (SEM) micrographs were recorded on a Hitachi SU8010 Scanning Electron Microscope. Transmission electron microscope (TEM) micrographs were recorded on a Hitachi HT7700 120 kV Compact-Digital Transmission Electron Microscope. Energy dispersive X-ray spectra (EDS) elemental mapping were acquired using a JEOL JEM-1400plus (120 kV). Powder X-ray diffraction (PXRD) patterns were obtained on a Rigaku SmartLab SE X-Ray Powder Diffractometer with Cu Kα line focused radiation (λ = 1.5405 Å) from 2θ = 2.00° up to 50.00° with 0.01° increment. Nitrogen adsorption isotherms were measured at 77 K with a Micromeritics ASAP2020 HD88 Surface Area and Porosity Analyser. Zeta potential was measured using Malvern Zetasizer Nano ZS90 System. Laser scanning confocal fluorescence images were captured with a Leica TCS SP8 Confocal Las er Scanning Microscopy with an objective lens (×20). The content of H_2O_2 was obtained by Full-wavelength, multi-channel microporous plate detector-SpectraMax 190 optical absorption marker. Thermogravimetric analysis (TGA) was obtained by Mettler Toledo TGA2 thermogravimetric analyzer. All fluorescence measurements were performed on an F-4600 spectrofluorometer (Hitachi, Japan) equipped with a circulating water bath for temperature control. X-ray photoelectron spectroscopy (XPS) was performed using an ESCALAB 250 X-ray photoelectron spectrometer with a monochromatized Al Kα X-ray source (1486.71 eV).

2. Synthesis of COF, **enzyme@COF** and HRP-COF

Synthesis of COF. COF was synthesized using a previously reported method with some modifications.[1] In brief, 1,3,5-tris(4-aminophenyl)benzene (TPB) (6 mg, 0.0168 mmol) and 2,5-dimethoxyterephthaldehyde (DMTP) (4.8 mg, 0.0288 mmol) were dispersed in a mixture of glacial acetic acid (0.3 mL) and H_2O (12 mL) under stirring at 25°C for 24 hours. Afterward, the resulting mixture was centrifuged, and the yellow powder obtained was washed several times with acetonitrile. Yield: 3.7 mg. FT-IR (ATR, cm^{-1}): 3369 (w), 2961 (w), 2940 (w), 2832 (w), 1679 (w), 1615 (m), 1592 (m), 1505 (m), 1488 (m), 1465 (m), 1410 (s), 1375 (m), 1290 (m), 1210 (s), 1181 (w), 1145 (m), 1040 (m), 1014 (w), 976 (w), 927 (w), 878 (w), 829 (m), 735 (w), 695 (w), 608 (w), 539 (w).

Synthesis of enzyme@COF. Firstly, 4.8 mg (0.0288 mmol) of 2,5-dimethoxyterephthaldehyde (DMTP) and 3 mg of enzyme were separately dissolved in 6 mL of H_2O and 3 mL of H_2O, respectively. The two solutions were mixed and stirred for 1 hour. Next, 6 mg (0.0168 mmol) of 1,3,5-tris(4-aminophenyl)benzene (TPB) was dissolved in 6 mL of H_2O, and 0.3 mL of acetic acid was added to the solution. This TPB solution was then added into the DMTP/enzyme solution, and the resulting mixture was stirred at room temperature for 24 hours. After completion of the reaction, the precipitate was collected by centrifugation and washed with water three times. **HRP@COF**: Yield: ~ 4.4 mg. FT-IR (ATR, cm^{-1}): 3306 (m), 2999 (w), 2939 (w), 2868 (w), 1678 (m), 1620 (m), 1593 (w), 1505 (w), 1486 (m), 1464 (w), 1409 (s), 1392 (w), 1288 (m), 1211 (s), 1162 (w), 1139 (w), 1085 (w), 1038 (m), 975 (w), 911 (w), 880 (w), 831 (m), 735 (w), 692 (w), 662 (w), 607 (w), 586 (w), 540 (w). **Pancreatin@COF**: Yield: ~ 6.0 mg. FT-IR (ATR, cm^{-1}): 3334 (w), 2939 (w), 2869 (w), 1678 (m), 1620 (m), 1593 (w), 1505 (w), 1484 (m), 1464 (w), 1409 (s), 1393 (w), 1292 (m), 1211 (s), 1129 (m), 1035 (m), 976 (w), 877 (m), 831 (m), 736 (w), 692 (w), 660 (m), 609 (w), 539 (w). **Lysozyme@ COF**: Yield: ~ 5.7 mg. FT-IR (ATR, cm^{-1}): 3352 (w), 2999 (w), 2939 (w), 2865 (w), 1681 (m), 1616 (m), 1592 (m), 1505 (w), 1486 (m), 1464 (m), 1408 (s), 1392 (w), 1288 (m), 1210 (s), 1181 (w), 1140 (m), 1038 (m), 1013 (w), 973 (w), 911 (w), 878 (w), 829 (m), 736 (w), 692 (m), 608 (w), 540 (w). **Urease@COF**： ~ 5.5 mg. FT-IR (ATR, cm^{-1}): 3343 (w), 2999 (w), 2940 (w), 2862 (w), 1680 (m), 1617 (m), 1591 (m), 1504 (w), 1485 (m), 1465 (m), 1408 (s), 1391 (w), 1288 (m), 1209 (s), 1181 (w), 1140 (m), 1037 (m), 1013 (w), 975 (w), 924 (w), 878 (w), 828 (m), 734 (w), 693 (m), 661 (w), 609 (w), 539 (w). **Ribonuclease A@COF**: Yield: ~ 5.2 mg. FT-IR (ATR, cm^{-1}): 3431 (w), 3353 (w), 2941 (w), 2866 (w), 1679 (m), 1617 (m), 1592 (m), 1506 (w), 1485 (m), 1465 (m), 1409 (s), 1392 (w), 1289 (m), 1211 (s), 1177 (w), 1139 (m), 1037 (m), 1013 (w), 976 (w), 912 (w), 877 (w), 829 (m), 734 (w), 692 (w), 661 (w), 609 (w), 539 (w). **Lipase@COF**: Yield: ~ 5.2 mg. FT-IR (ATR, cm^{-1}): 3306 (w), 2998 (w), 2939 (w), 2867 (w), 1679 (m), 1618 (m), 1592 (w), 1505 (w), 1485 (m), 1465 (m), 1409 (s), 1392 (w), 1289 (m), 1211 (s), 1181 (w), 1140 (m), 1037 (m), 1013 (w), 976 (w), 911 (w), 877 (w), 830 (m), 736 (w), 692 (w), 661 (w), 609 (w), 539 (w). **Trypsin@COF**: Yield: ~ 6.4 mg. FT-IR (ATR, cm^{-1}): 3356 (w), 3000 (w), 2937 (w), 2864 (w), 1679 (m), 1617 (m), 1592 (m), 1505 (w), 1486 (m), 1464 (m), 1408 (s), 1392 (w), 1288 (m), 1210 (s), 1180 (w), 1140 (m), 1038 (m), 1013 (w), 974 (w), 915 (w), 878 (w), 829 (m), 734 (w), 692 (m), 608 (w), 537 (w). **GOx@COF**: Yield: ~ 6.0 mg. FT-IR (ATR, cm^{-1}): 3288 (m), 2957 (w), 2938 (w), 2877 (w), 1651 (m), 1620 (m), 1592 (w), 1506 (m), 1488 (w), 1465 (m), 1409 (s), 1289 (m), 1211 (s), 1179 (w), 1143 (m), 1101 (w), 1040 (m), 1013 (w), 975 (w), 928 (w), 878 (w), 828 (m), 734 (w), 695 (m), 607 (w), 539 (w).

Preparation of HRP-COF. To immobilize biomolecules using the adsorption method,[2] 3 mg of COF was added directly to a solution containing 1.0 mg mL^{-1} of HRP in 0.1 M MES buffer (pH 7.0). The resulting mixture was then centrifuged, and the precipitate was washed with water three times. Yield: 3.67 mg. FT-IR (ATR, cm^{-1}): 3355 (w), 2961 (w), 2938 (w), 2832 (w), 1682 (m), 1653 (w), 1617 (m), 1593 (m), 1506 (m), 1488 (m), 1465 (m), 1410 (s), 1374 (w), 1289 (m), 1211 (s), 1181 (w), 1143 (m), 1039 (m), 1014 (w), 975 (w), 924 (w), 879 (w), 830 (m), 736 (w), 694 (w), 609 (w), 537 (w).

3. Synthesis of ZIF-8 and HRP@ZIF-8

Synthesis of ZIF-8. The pure ZIF-8 nanocrystals was synthesized using a previously reported method with some modifications.[3] $Zn(NO_3)_2$ water solution (0.31 M, 1 mL) was added into 2-methylimidazole water solution (2-MIM, 1.25 M, 10 mL) under stirring at 25 ℃. After stirring for about 30 min, the product was collected by centrifuging at 6000 rpm for 10 min, and washed with water for three times. Yield: 53.76 mg. FT-IR (ATR, cm^{-1}): 3628 (w), 3132 (w), 3099 (w), 2952 (w), 2926 (w), 1567 (w), 1508 (w), 1457 (m), 1424 (m), 1381 (w), 1309 (m), 1179 (m), 1145 (s), 1106 (w), 994 (m), 953 (w), 846 (w), 759 (m), 693 (w), 685 (w), 421 (s).

Synthesis of HRP@ZIF-8. A water solution (1 mL) of HRP (7.5 mg mL^{-1}), and $Zn(NO_3)_2$ water solution (0.31 M, 1 mL) were mixed with 2-methylimidazole water solution (2-MIM, 1.25 M, 10 mL) under stirring at 25 ℃. After stirring for about 30 min, the product was collected by centrifuging at 6000 rpm for 10 min, and washed with water for three times. Yield: 30 mg. FT-IR (ATR, cm^{-1}): 3269 (w), 3132 (w), 3099 (w), 2953

(w), 2927 (w), 1652 (w), 1565 (w), 1508 (w), 1457 (m), 1425 (m), 1382 (w), 1309 (m), 1179 (m), 1145 (s), 1106 (w), 994 (m), 953 (w), 846 (w), 759 (m), 693 (w), 684 (w), 421 (s).

4. Synthesis of COF@MnO_2, **GOx&HRP@COF** and **GOx&HRP@COF@MnO_2**

Synthesis of GOx&HRP@COF. Firstly, 4.8 mg (0.0288 mmol) of 2,5-dimethoxyterephthaldehyde (DMTP) and 3 mg of enzyme (GOx, 1.5 mg; HRP, 1.5 mg) were separately dissolved in 6 mL of H_2O and 3 mL of H_2O, respectively. The two solutions were mixed and stirred for 1 hour. Next, 6 mg (0.0168 mmol) of 1,3,5-tris(4-aminophenyl)benzene (TPB) was dissolved in 6 mL of H_2O, and 0.3 mL of acetic acid was added to the solution. This TPB solution was then added into the DMTP/enzyme solution, and the resulting mixture was stirred at room temperature for 24 hours. After completion of the reaction, the precipitate was collected by centrifugation and washed with water three times. Yield: 4.2 mg. FT-IR (ATR, cm^{-1}): 3337 (w), 2916 (w), 2870 (w), 1670 (m), 1616 (m), 1590 (w), 1507 (w), 1481 (m), 1472 (m), 1409 (m), 1394 (m), 1296 (m), 1211 (m), 1128 (m), 1030 (m), 877 (m), 830 (m), 736 (s), 692 (s), 658 (m), 609 (s), 527 (s).

Synthesis of COF@MnO_2. COF@MnO_2 was synthesized using a previously reported method with some modifications.[4] Briefly, 2 mg COF was dispersed in aqueous solution containing $KMnO_4$ (200 μM, 10 mL) and ultrasonic for 30 min. After completion of the reaction, the precipitate was collected by centrifugation and washed with water three times. Yield: 2.1 mg. FT-IR (ATR, cm^{-1}): 3346 (m), 2964 (w), 2869 (w), 1678 (m), 1616 (m), 1592 (w), 1505 (w), 1485 (m), 1464 (m), 1409 (m), 1393 (m), 1289 (m), 1211 (m), 1140 (m), 1037 (m), 877 (m), 830 (m), 736 (s), 693 (s), 660 (m), 609 (s), 527 (s), 471 (m).

Synthesis of GOx&HRP@COF@MnO_2. Briefly, 2 mg **GOx&HRP@COF** was dispersed in aqueous solution containing $KMnO_4$ (200 μM, 10 mL) and ultrasonic for 30 min. After completion of the reaction, the precipitate was collected by centrifugation and washed with water three times. Yield: 2.1 mg. FT-IR (ATR, cm^{-1}): 3362 (m), 2941 (w), 2870 (w), 1668 (m), 1616 (m), 1592 (w), 1505 (w), 1487 (m), 1465 (m), 1410 (m), 1394 (m), 1290 (m), 1212 (m), 1143 (m), 1038 (m), 877 (m), 830 (m), 736 (s), 693 (s), 660 (m), 609 (s), 527 (s), 471 (m).

5. Confocal imaging

To label enzymes with fluorescent molecules, 4 mg of rhodamine B (RhB) was dissolved in 2 mL of dimethyl sulfoxide (DMSO) at a concentration of 2 mg mL^{-1}. This solution was slowly added to 2 mL of horseradish peroxidase (HRP) solution at a concentration of 5 mg mL^{-1} in a 0.5 M, pH 9.5 carbonate buffer. The resulting mixture was shaken for 6 hours at 300 rpm and at ambient temperature in the dark. To remove any free RhB, the solution was dialyzed against deionized water. The RhB-labeled HRP was then freeze-dried and dissolved in water for the subsequent synthesis of the **RhB-HRP@COF** composites. Laser scanning confocal microscope images were captured using a Leica TCS SP8 Confocal Laser Scanning Microscope with a ×20 objective lens. The detection wavelengths for RhB were 561 nm.

6. The loading capacity of **enzyme@COF** composites

Fluorescein isothiocyanate (FITC) labeling of different enzymes: 4 mg of fluorescein isothiocyanate (FITC) was dissolved in 2 mL of dimethyl sulfoxide (DMSO) at a concentration of 2 mg mL^{-1}. This solution was slowly added to 2 mL of various enzymes solution at a concentration of 5 mg mL^{-1} in a 0.5 M, pH 9.5 carbonate buffer, including glucose oxidase (GOx), ribonuclease A, lipase, lysozyme, trypsin, pancreatin, and urease. The resulting mixture was shaken for 6 hours at 300 rpm and at ambient temperature in the dark. To remove any free FITC, the solution was dialyzed against deionized water. The fluorescent molecule-labeled enzymes were then freeze-dried and stored at 4 ℃ until further use.

Calculation of the loading capacity of FITC labelled enzymes. Fluorescein isothiocyanate (FITC) labeled enzyme solutions with different concentrations were prepared, and the fluorescence spectra from 425-700 nm (with excitation at 406 nm) were recorded using a fluorescence spectrometer. The **FITC-enzyme@COF** was synthesized using the same method as for preparing **enzyme@COF**. After centrifugation, the supernatant and all washing solutions were collected to measure the loading capacity. The loading capacity was calculated using the following

equation: ($M_{initial\ drug}$ - $M_{drug\ in\ supernatant}$) / $M_{nanoparticles}$. The FITC-**GOx&**RhB-**HRP@COF@MnO_2** was synthesized using the same method as for preparing **GOx&HRP@COF@MnO_2**. After centrifugation, the supernatant and all washing solutions were collected to measure the loading capacity. The loading capacity was calculated using the following equation: ($M_{initial\ drug}$ - $M_{drug\ in\ supernatant}$) / $M_{nanoparticles}$.

Calculation of the loading capacity and of HRP labelled enzymes. Different concentrations of RhB-HRP solutions (0.1, 0.2, 0.3, 0.4, 0.5, 0.6 mg mL^{-1}) were prepared and their fluorescence spectra from 380-700 nm (with excitation at 359 nm) were recorded. The **RhB-HRP@COF** was synthesized using the **enzyme@COF** preparation method, and the supernatant and all washing solutions were collected after centrifugation to determine the loading capacity. The loading capacity was calculated using the following equation: ($M_{initial\ drug}$ - $M_{drug\ in\ supernatant}$) / $M_{nanoparticles}$. The FITC-**GOx&**RhB-**HRP@COF@MnO_2** was synthesized using the same method as for preparing **GOx&HRP@COF@MnO_2**. After centrifugation, the supernatant and all washing solutions were collected to measure the loading capacity. The loading capacity was calculated using the following equation: ($M_{initial\ drug}$ - $M_{drug\ in\ supernatant}$) / $M_{nanoparticles}$.

7. Catalytic activities of **enzyme@COF**

Detection of pH value. To evaluate the performance of **GOx@COF**, an aqueous solution of **GOx@COF** (200 μg mL^{-1}, 5 mL) was incubated with different concentrations of glucose (0, 1, 2, 3, 4, 5 mmol L^{-1}) at 37 °C for 30 min. The pH value was then measured using a digital pH meter. For **GOx&HRP@COF**, an aqueous solution of **GOx&HRP@COF** (800 μg mL^{-1}, 4 mL) was incubated with different concentrations of glucose (0, 0.1, 0.2, 0.3, 0.4, 0.5 mol L^{-1}) at 37 °C for 150 min.

Detection of H_2O_2 concentration. To determine the activity of **GOx@COF**, a solution containing 200 μg mL^{-1} of **GOx@COF** (5 mL) was incubated with different concentrations of glucose (0, 0.1, 0.2, 0.3, 0.4, 0.5 mol L^{-1}) at 37 °C for 150 minutes. The supernatant was collected and analyzed using the Hydrogen Peroxide Assay Kit (Beyotime Biotechnology Co., Ltd.). The same experimental procedure was applied to assess the activity of **GOx&HRP@COF** (200 μg mL^{-1}).

Enzymatic activity of HRP. The activity of HRP was measured using a colorimetric assay of 3,3',5,5'-tetramethylbenzidine (TMB). A mixture of 500 μL of **HRP@COF** (400 μg mL^{-1}), 5 μL of H_2O_2 solution (10 mM, final concentration: 0.1 mM), and 50 μL of TMB solution (10 mM, final concentration: 1 mM) was prepared. For the control group, 50 μL of TMB solution (10 mM, final concentration: 1 mM) was mixed with 450 μL of PBS buffer solution (pH = 5.5). The absorption spectra of these samples were then recorded at various time points using a UV-Vis Spectrometer. The same experimental procedure was applied to assess the activity of **GOx&HRP@COF**, where 400 μg mL^{-1} of **GOx&HRP@COF** was reacted with different concentrations of H_2O_2 solution (0, 5, 10, 20, 50 mM).

The Michaelis-Menten constant was calculated based on the Michaelis-Menten saturation curve. For each H_2O_2 concentration, the initial reaction rates (V_0) were calculated from the absorbance variation using the Beer-Lambert Law (Equation (1)) (ε=39000 $M^{-1}\cdot cm^{-1}$ for TMBox; c indicates the TMBox concentration; l=1 cm for the length of the solution in the light path). The reaction rates were then plotted against their corresponding H_2O_2 concentration and then fitted with the Michaelis-Menten curves (Equation (2)) to determine the maximum reaction velocity (Vmax) and Michaelis constant (Km).

$$A = \varepsilon l c \quad (1)$$

$$V_0 = \frac{V_{max}\cdot[S]}{[s] + K_m} \quad (2)$$

Bioactivity of HRP@COF. The activity of HRP was determined by measuring the rate of hydrogen peroxide decomposition using pyrogallol as the hydrogen donor, which produces a yellowish product called purpurogallin.[5] For the assay, a solution containing 76 μL of KH_2PO_3 (100 mM, pH 6.0), 38 μL of H_2O_2 (5% w/w in deionized water), 76 μL of pyrogallol (5% w/w in deionized water), and 1.8 mL of PBS buffer (pH 7.4) was prepared (solution A). **HRP@COF** were added to solution A, and the absorbance of the solution was monitored at 420 nm using a UV-Vis spectrophotometer

at 30-second intervals. To ensure consistency, the amount of free enzyme used in the enzymatic activity assay was adjusted to match the amount of enzyme loaded into **HRP@COF**, as determined from the loading capacity.

8. Cascading catalytic reaction of **GOx&HRP@COF**

The **GOx&HRP@COF** with a final concentration of 0, 0.1, 0.2, 0.4, and 0.8 mg mL^{-1} was prepared from a stock concentration of 4 mg mL^{-1}. Then, 100 μL of a glucose solution (with a final concentration of 40 mM) and 100 μL of a TMB (3,3',5,5'-tetramethylbenzidine) solution (with a final concentration of 1 mM) were added into. The absorption spectra of these sample solutions, spanning the wavelength range of 500-800 nm, were finally recorded using an ultraviolet-visible spectrometer.

9. Catalytic performance of **GOx&HRP@COF@MnO_2**

Influence of GSH. Synthesis of FITC-**GOx&HRP@COF** and FITC-**GOx&HRP@COF@MnO_2** with FITC-labeled GOx. The fluorescence spectra of FITC-**GOx&HRP@COF** (400 μg mL^{-1}), FITC-**GOx&HRP@COF@MnO_2** (400 μg mL^{-1}) and GSH (0.5 mM) -treated FITC-**GOx&HRP@COF@MnO_2** solutions (400 μg mL^{-1}) from 425-700 nm (with excitation at 406 nm) were recorded using a fluorescence spectrometer.

Influence of pH. FITC-**GOx&HRP@COF@MnO_2** solution (400 μg mL^{-1}) reacted with GSH (0.5 mM) at different pH (5.5, 7.0), and the fluorescence spectra from 425-700 nm (with excitation at 406 nm) were recorded using a fluorescence spectrometer.

Influence of GOx's concentrations. A mixture of different concentrations of **GOx&HRP@COF@MnO_2** (0, 25, 50, 75, 100 μL) (4 mg mL^{-1}, final concentration: 0, 0.1, 0.2, 0.3. 0.4 mg mL^{-1}) treated with GSH (0.5 mM) 15 min, 100 μL of glucose solution (200 mM, final concentration: 20 mM), and 100 μL of TMB solution (10 mM, final concentration: 1 mM) was added. The absorption spectra of these samples at 500-800 nm were then recorded with an ultraviolet-visible spectrometer.

Enhanced catalytic performance. When Using MB as catalyst substrate, the catalytic activities of the following solutions were compared: MB (10 μg mL^{-1}); MB (10 μg mL^{-1}) + H_2O_2 (8 mM); MB (10 μg mL^{-1}) + glucose (50 mM); MB (10 μg mL^{-1}) + COF@MnO_2 (0.4 mg mL^{-1}) + GSH (0.5 mM) + H_2O_2 (8 mM); MB (10 μg mL^{-1}) + **GOx&HRP@COF** (0.4 mg mL^{-1}) + glucose (50mM); MB (10 μg mL^{-1}) + **GOx&HRP@COF@MnO_2** (0.4 mg mL^{-1}) + GSH (0.5 mM) + glucose (50 mM). The absorption spectra of these samples at 400-800 nm were then recorded with an ultraviolet-visible spectrometer.

10. Validation of the in vitro antitumor efficacy of **GOx&HRP@COF@MnO_2**

Cellular Uptake. 4T1 cells (1.5×10^5) were seeded into confocal dishes and incubated overnight. Subsequently, the cells were exposed to fresh cell culture medium (200 μL) containing FITC labeled **GOx&HRP@COF@MnO_2** (200 μg mL^{-1}) and incubated for different times (0 h, 1 h, 2 h and 4 h). After this incubation period, the cells were washed with DPBS three times to remove any excess materials. The nucleus was counterstained with Hoechst 33342 and observed using confocal laser microscope at 405 and 488 nm excitation.

Lysosome Colocalization Test. 4T1 cells (2.5×10^5) were seeded into confocal dishes and allowed to culture overnight. After discarding the culture medium, the cells were exposed to a cell culture medium containing FITC labeled **GOx&HRP@COF@MnO_2** (200 μg mL^{-1}) and incubated for different times (0 h, 2 h, 4 h and 6 h). Afterward, the cells were washed three times with HHBS and preheated Lyso-Tracker Red was added to the cells and incubated for 30 min at 37 °C. The lysosomes were labeled with red fluorescence and imaged by the confocal laser microscope at 488 and 543 nm excitation.

Mitochondrion Colocalization Test. 4T1 cells (2.5×10^5) were seeded into confocal dishes and allowed to culture overnight. After discarding the culture medium, the cells were exposed to a cell culture medium containing FITC labeled **GOx&HRP@COF@MnO_2** (200 μg mL^{-1}) and incubated for different times (0 h, 2 h, 4 h and 6 h). Afterward, the cells were washed three times with DPBS and preheated Mito-Tracker Red was added to

the cells and incubated for 30 min at 37 °C. The mitochondrion was labeled with red fluorescence and imaged by the confocal laser microscope at 488 and 543 nm excitation.

MTT Experiment. The samples cytotoxicity was estimated using standard MTT assay against cancer cells (4T1 cells) and normal cells (HL-7702 cells). First, the HL-7702 or 4T1 cells were seeded into a 96-well plate (2.5×10^5) and incubated for 12 h. They were then incubated with varying concentrations of COF, COF@MnO_2, **GOx&HRP@COF**, **GOx&HRP@COF@MnO_2** (0, 25, 50, 100, 150, 200, 400 μg mL^{-1}) for 24 h. Then MTT (100 μL, 0.5 mg mL^{-1}) solution was added into each well. After incubated at 37 °C for 4 h, the remaining MTT solution was removed and the DMSO (150 μL) was added to each well to dissolve the formazan crystals. The absorbance intensity at 490 nm was recorded by Microplate reader.

Intracellular GSH content measuring. 4T1 cells (4×10^5) were seeded into 6-well plates and incubated overnight. Subsequently, the cells were exposed to fresh cell culture medium (200 μL) containing COF, COF@MnO_2, **GOx&HRP@COF**, **GOx&HRP@COF@MnO_2** (200 μg mL^{-1}) and incubated for 12 h, respectively. The cells were incubated with NEM (N-ethylmaleimide) for 10 min. After digestion, the cells were dispersed in 100 μL 3% Titonx-100, placed at 4℃ for 24h, and centrifuged at 12 000 rpm for 10 min. 40 μL H_2O and 10 μL 0.4 mg mL^{-1} DTNB (5,5' -dithiobis (2-nitrobenzoic acid)) were added into the 50 μL supernatant, and the absorbance at 412 nm was measured by enzyme spectrometer. DTNB interacts with GSH, leading to the generation of TNB, with the characteristic absorption peak intensity of TNB at 412 nm increasing as the concentration of GSH rises.

Intracellular pH Changes. 4T1 cells (2.5×10^5) were seeded into confocal dishes and incubated overnight. Subsequently, the cells were exposed to fresh cell culture medium (200 μL) containing COF, COF@MnO_2, **GOx&HRP@COF**, **GOx&HRP@COF@MnO_2** (200 μg mL^{-1}) and incubated for 12 h, respectively. After this incubation period, the cells were washed with DPBS three times to remove any excess materials. Then, BCECF AM was added and the cells were stained for 30 min at 37 °C. Then, the cells images were observed by confocal microscopy at 488 nm excitation.

Intracellular ROS production. 4T1 cells (2.5×10^5) were seeded into confocal dishes and incubated overnight. Subsequently, the cells were exposed to fresh cell culture medium (200 μL) containing COF, COF@MnO_2, **GOx&HRP@COF**, **GOx&HRP@COF@MnO_2** (200 μg mL^{-1}) and incubated for 12 h, respectively. After this incubation period, the cells were washed with DPBS three times to remove any excess materials. Then, DCFH-DA was added and the cells were stained for 30 min at 37 °C. Then, the cells images were observed by confocal microscopy at 488 nm excitation.

Intracellular mitochondrial membrane potential changes. 4T1 cells (2.5×10^5) were seeded into confocal dishes and incubated overnight. Subsequently, the cells were exposed to fresh cell culture medium (200 μL) containing COF, COF@MnO_2, **GOx&HRP@COF**, **GOx&HRP@COF@MnO_2** (200 μg mL^{-1}) and incubated for 12 h, respectively. After this incubation period, the cells were washed with DPBS three times to remove any excess materials. Then, JC-1 solution was added and the cells were stained for 30 min at 37 °C. Then, the cells images were observed by confocal microscopy at 488 and 543 nm excitation.

Intracellular ATP content measuring. 4T1 cells (4×10^5) were seeded into 6-well plates and incubated overnight. Subsequently, the cells were exposed to fresh cell culture medium (200 μL) containing COF, COF@MnO_2, **GOx&HRP@COF**, **GOx&HRP@COF@MnO_2** (200 μg mL^{-1}) and incubated for 12 h, respectively. Then, the cells were lysed and then centrifuged at 12 000 rpm for 5 min. 100 μLATP was added into 20 μL supernatant to detect the working liquid. The microplate reader detects ATP levels by recording supernatant luminescence.

11. Validation of the in vivo antitumor efficacy of **GOx&HRP@COF@MnO_2**

In vivo antitumor therapy. The mice were used when the tumor size reached approximately 100 mm^3, and were then randomly divided into five groups: I: PBS; II: COF; III: COF@MnO_2; IV: **GOx&HRP@COF**; V: **GOx&HRP@COF@MnO_2**. The mice were administered with a dose of **GOx&HRP@COF@MnO_2** (10 mg kg^{-1}). The tumor volume and body weight of the mice were recorded daily for 14 days during the experiment. At the end of the treatment process, the mice were sacrificed, and the major organs were collected for histological analysis. Specifically, these organs

were fixed in 10% paraformaldehyde solution, and prepared to slice in process routinely. Then the slices were stained with hematoxylin and eosin and observed by a fluorescence microscopy. Tumor volume = (length×width^2)/2.

Hemolytic test. Blood is first collected from the eyeball and washed with DPBS until the supernatant is colorless. Different concentrations (0, 12.5, 25, 50, 75, 100, 150, 200, 400 μg mL^{-1}) of **GOx&HRP@COF@MnO$_2$** solution were incubated with blood for 4 h, DPBS and purified water were used as control group. After centrifuging the sample at 4000 rpm for 5 min, the supernatant was measured using a microplate reader.

12. Statistical analysis

The statistical comparison between two groups were analyzed by two-tailed student T-test, and multigroup comparisons were conducted using a one-way ANOVA with Tukey's post hoc test. All statistical analyses were performed using the GraphPad Prism 8 software, n=3 samples per group. Significance was indicated as follows: *p < 0.05, **p < 0.01, ***p < 0.001 or ****p < 0.0001. Error bar represents standard deviation (SD).

13. Ethical approval

The animal experiment was carried out according to the guidelines of the National Regulation of China for Care and Use of Laboratory Animals and approved by the Ethics Committee of Shandong Normal University (AEECSDNU2023067).

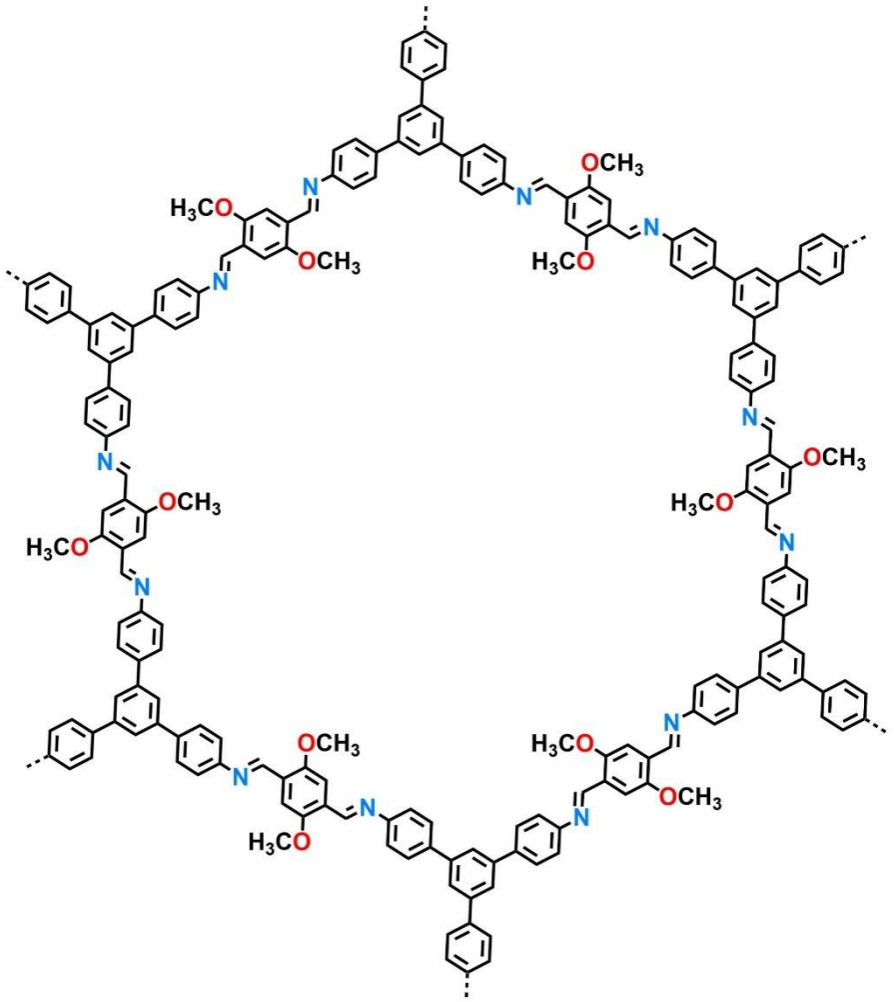

Fig. S1 The chemical structure of COF DMTP-TPB.

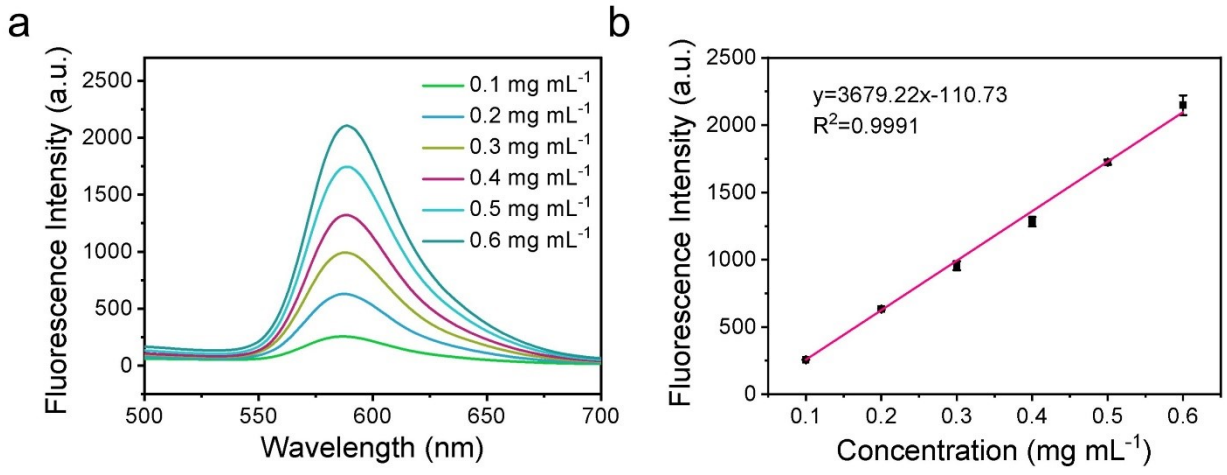

Fig. S2 Standard curve of RhB-HRP. (a) Fluorescence spectra of RhB-HRP with different concentrations. (b) Linear relationships between the fluorescence intensity of RhB-HRP at 588 nm and the RhB-HRP concentration. The error bar is the standard deviation from the mean (n = 3).

Supplementary note 1: Discussion for Fig. S3 and S4

It is worth noting that the enzyme-loaded enzyme@COF showed distinctly different morphologies depending on the type of the enzymes, as shown in the transmission electron microscopy (TEM, Fig. S3, ESI†) and scanning electron microscopy (SEM, Fig. S4, ESI†) images. This observation suggests that the varying interactions between enzyme and COF might contribute to the diverse patterns of enzyme localization and aggregation, and this discovery unveils an exciting opportunity to tailor the property and enhance the performance of enzyme-immobilized COFs by considering the specific characteristics of the enzymes and the desired applications.

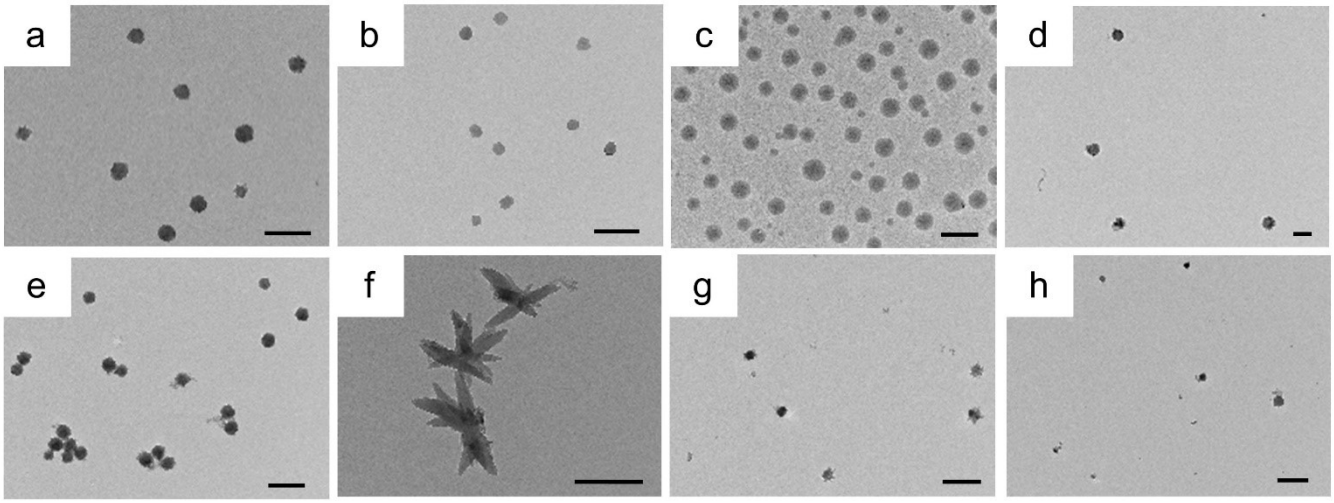

Fig. S3 Transmission electron microscopy (TEM) images showing enzyme@COF. (a) COF, (b) Pancreatin@COF, (c) Lysozyme@COF, (d) Urease@COF, (e) Ribonuclease A@COF, (f) Lipase@COF, (g) Trypsin@COF, (h) GOx@COF. Scale bars, 500 nm.

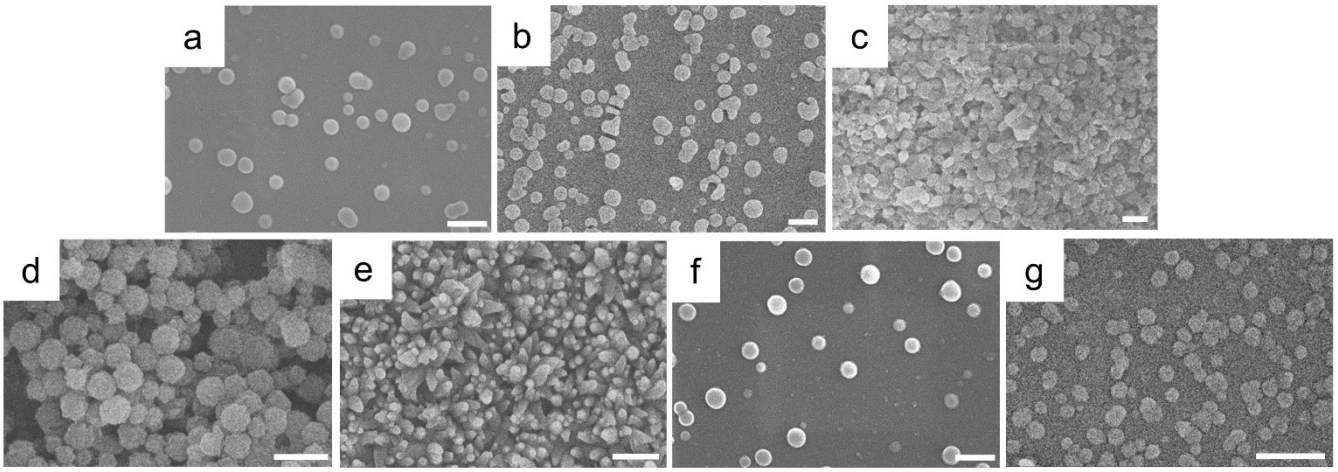

Fig. S4 SEM images of enzyme@COF composites. (a) Pancreatin@COF, (b) Lysozyme@COF, (c) Urease@COF, (d) Ribonuclease A@COF, (e) Lipase@COF, (f) Trypsin@COF, (g) GOx@COF. Scale bars, 500 nm.

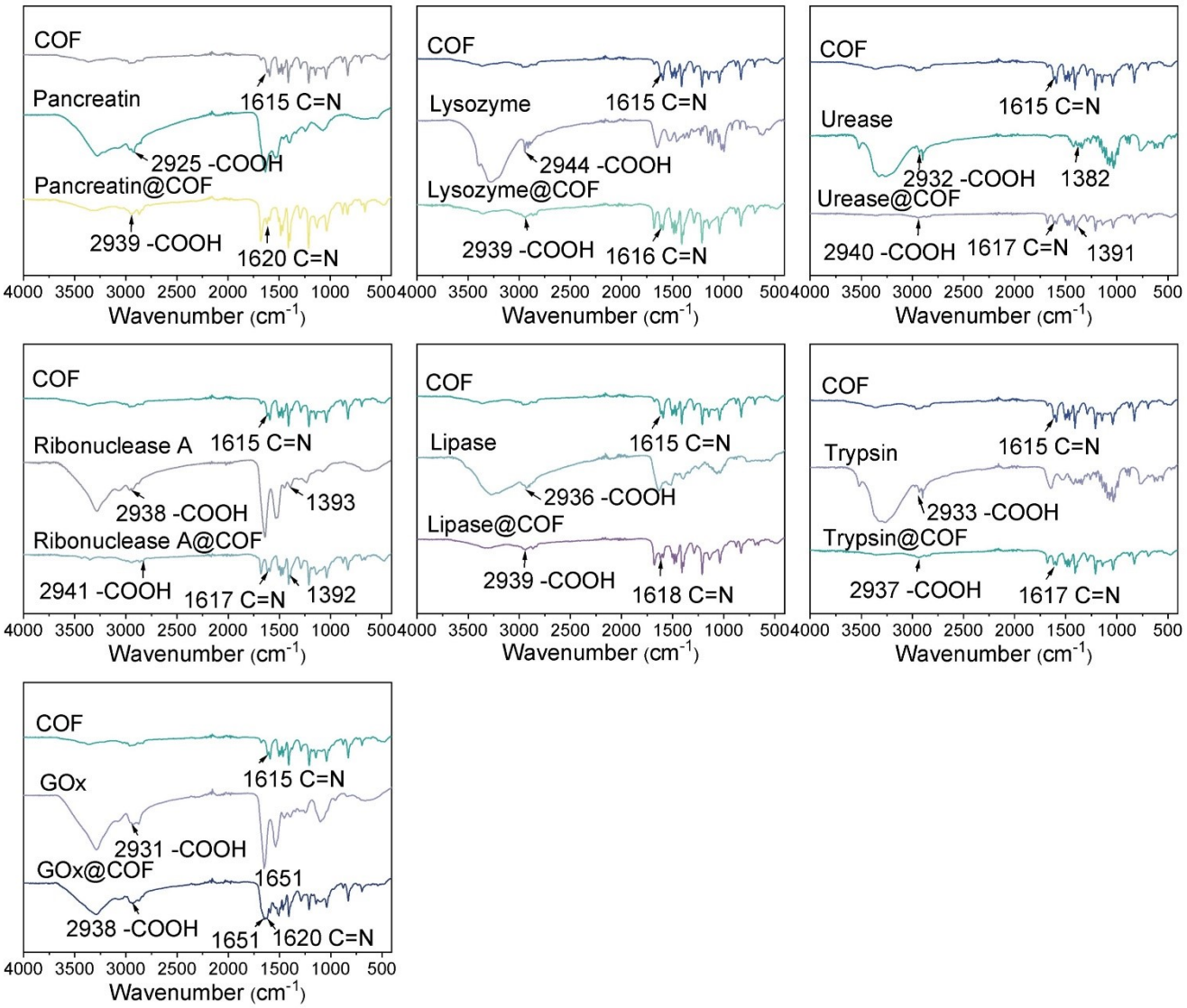

Fig. S5 FTIR spectra of various enzymes and enzyme@COF composites.

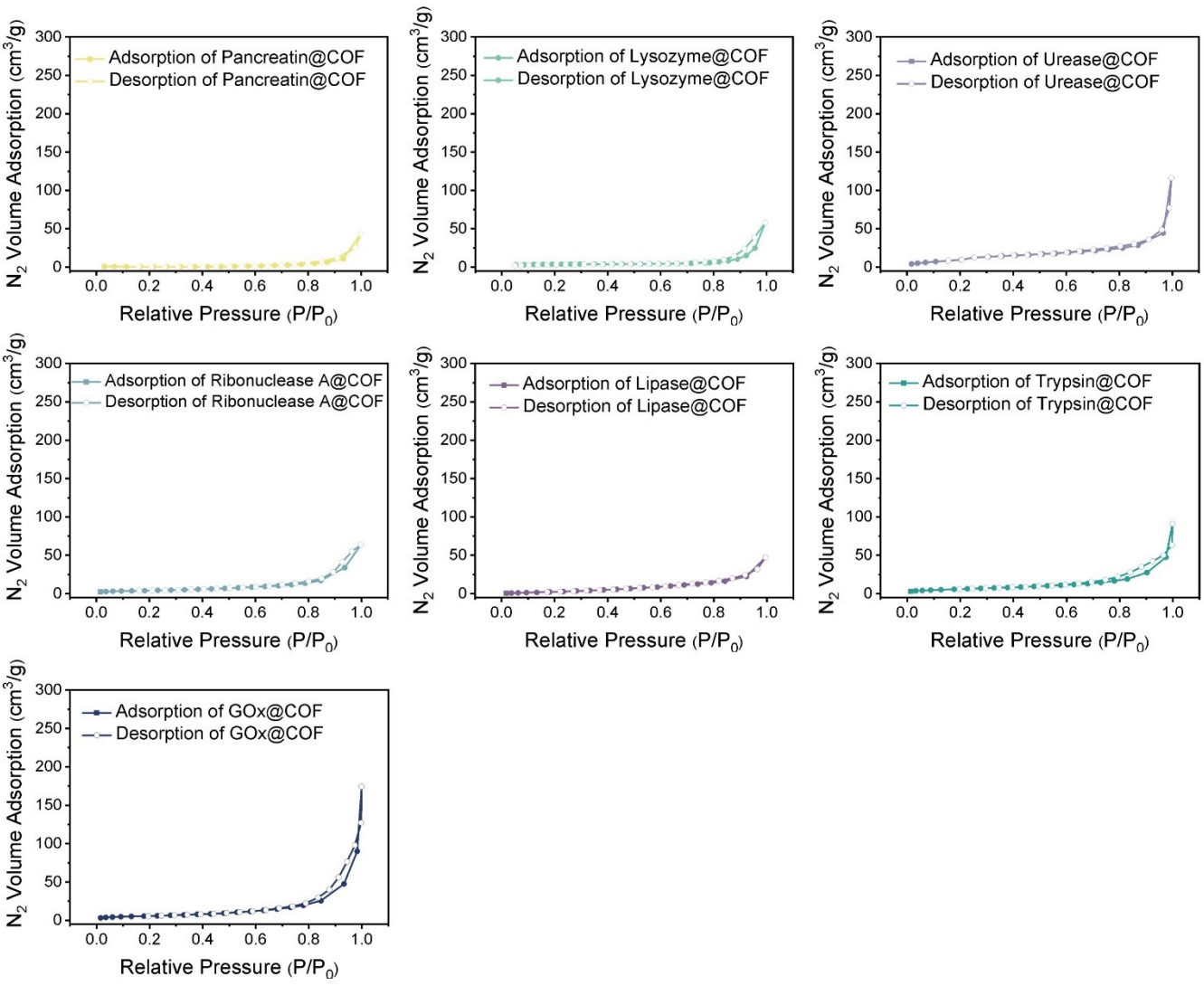

Fig. S6 N_2 adsorption-desorption isotherms of enzyme@COF composites.

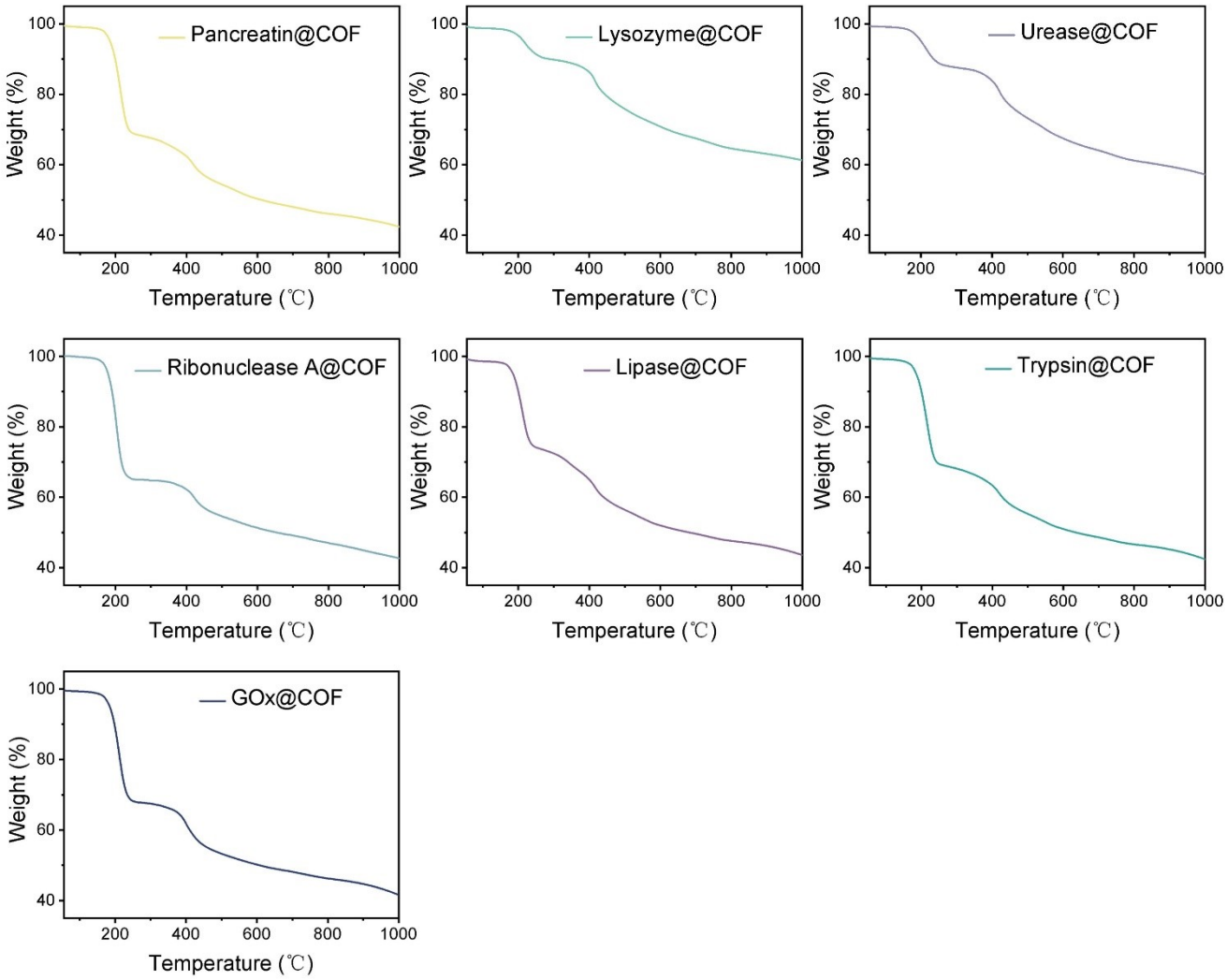

Fig. S7 TGA traces of enzyme@COF composites.

Table S1. The loading capacity of enzyme@COF composites.

Sample	Loading Capacity
HRP@COF	23.1 wt%
Pancreatin@COF	37.8 wt%
Lysozyme@COF	26.5 wt%
Urease@COF	29.9 wt%
Ribonuclease A@COF	37.9 wt%
Lipase@COF	39.3 wt%
Trypsin@COF	35.7 wt%
GOx@COF	35.5 wt%

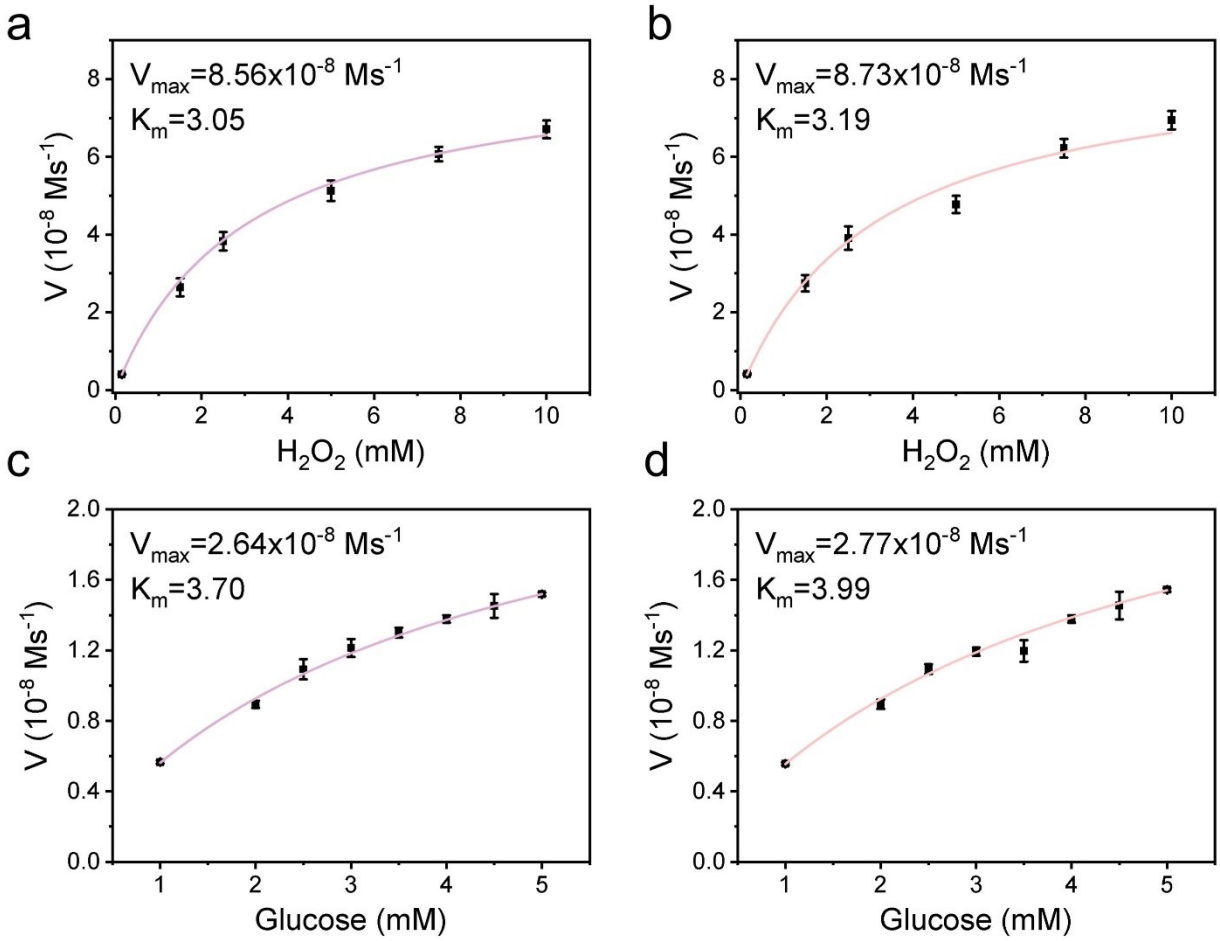

Fig. S8 Steady-state kinetic assay of natural enzymes and nanozymes. Typical Michaelis−Menten curves for (a) HRP, (b) HRP@COF, (c) GOx, and (d) GOx@COF.

Supplementary note 2: Discussion for Fig. S9

For example, the catalytic activity of immobilized HRP could be measured by monitoring the conversion of pyrogallol to purpurogallin in the presence of H_2O_2 based on the absorbance increase ratio at 420 nm.[5] As is shown, when proteolytic agent was added to a mixture of trypsin/HRP@COF or trypsin/HRP, the encapsulated HRP showed a relative activity of 78%. In contrast, the free HRP exhibited unsatisfactory catalytic performance, displaying a relative activity of only 26% (Fig. S9, ESI†). Furthermore, when HRP and HRP@COF were respectively immersed in boiling water and boiling dimethylformamide for 1 h, the free HRP retained only 5-6% relative activity, while HRP@COF maintained a relative activity of 74-76%.

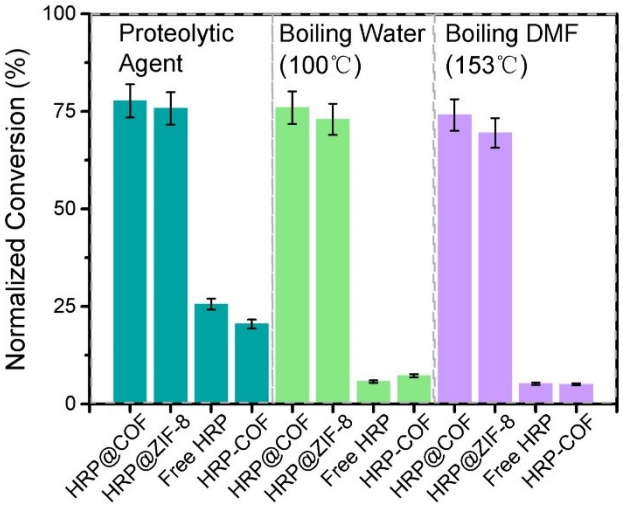

Fig. S9 The detection of HRP performance in different samples. Product conversion of free HRP, HRP@COF, HRP@ZIF-8, and HRP-COF in the presence of proteolytic agent, trypsin, after treatment in boiling water for 1 h, and after treatment in boiling dimethylformamide (DMF) for 1 h at 153 ℃, respectively. Data were normalized against free HRP activity at room temperature. The error bar is the standard deviation from the mean (n = 3).

Supplementary note 3: Discussion for Fig. S10 and S11

HRP@ZIF-8 was prepared by a coprecipitation method (Fig. S10, ESI†),[3] and HRP was embedded within the zeolitic imidazolate framework. HRP-COF was prepared via the traditional adsorption method (Fig. S11, ESI†), and most of the HRP molecules were located on the COF surface.[6] As expected, HRP@COF presented superior catalytic activity compared with HRP@ZIF-8 (75.8% in trypsin, 73.0% in boiling water, 69.5% in boiling DMF) and HRP-COF (20.5% in trypsin, 7.3% in boiling water, 5.1% in boiling DMF).

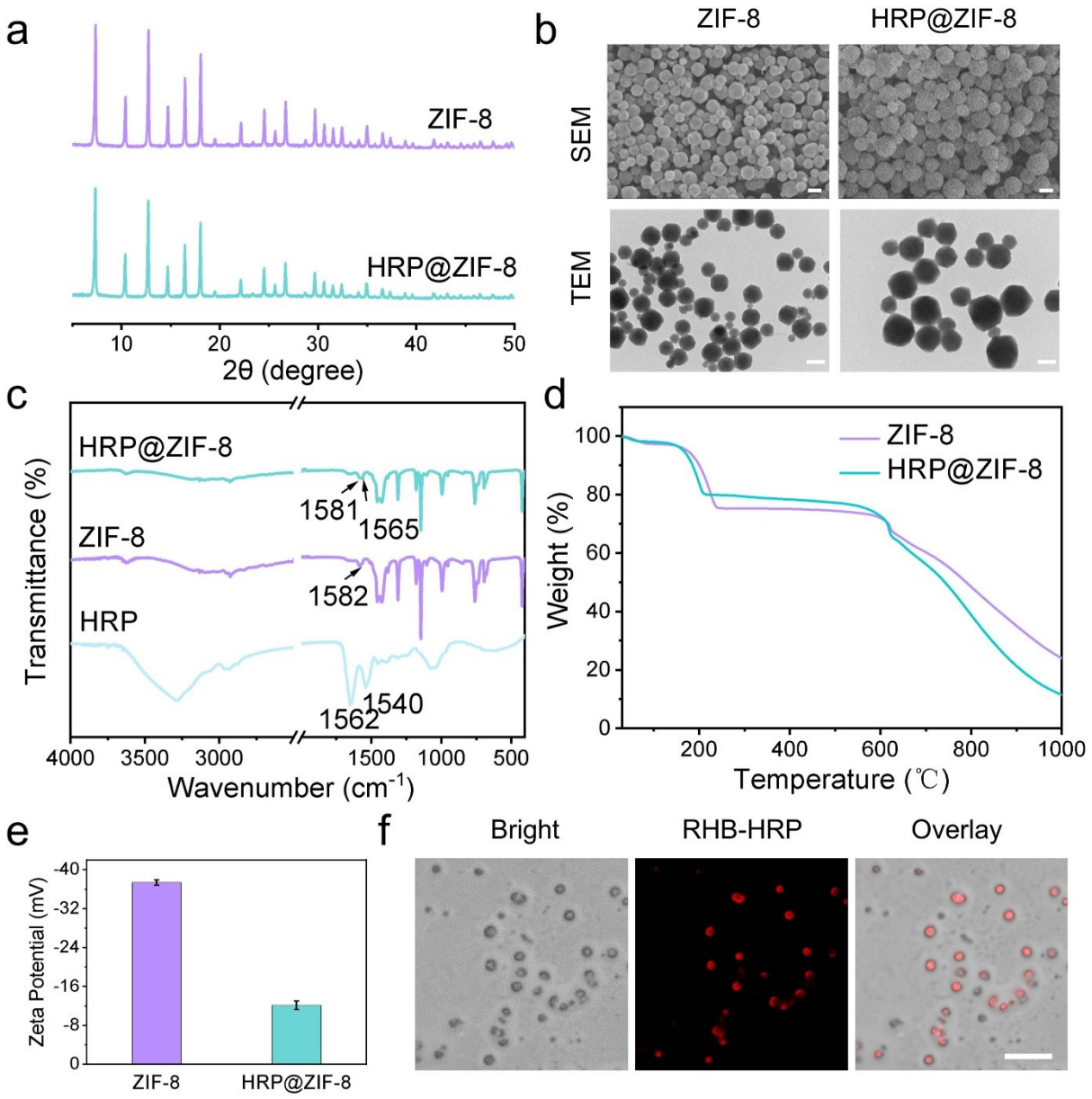

Fig. S10 Characterization of ZIF-8 and HRP@ZIF-8. (a) PXRD patterns of ZIF-8 and the HRP@ZIF-8 nanoparticles. (b) SEM and TEM images of the ZIF-8 and the HRP@ZIF-8 nanoparticles. Scale bars, 500 nm. (c) FTIR spectra of pure ZIF-8 crystal, HRP, and HRP@ZIF-8 nanoparticles. (d) TGA curves of ZIF-8 and HRP@ZIF-8 composite in air. (e) Zeta potentials of the ZIF-8 and HRP@ZIF-8 nanoparticles (NPs). The error bar is the standard deviation from the mean (n = 3). (f) Confocal microscopy image of the HRP@ZIF-8 composite, HRP was labeled with RhB (red). Scale bar, 2 μm.

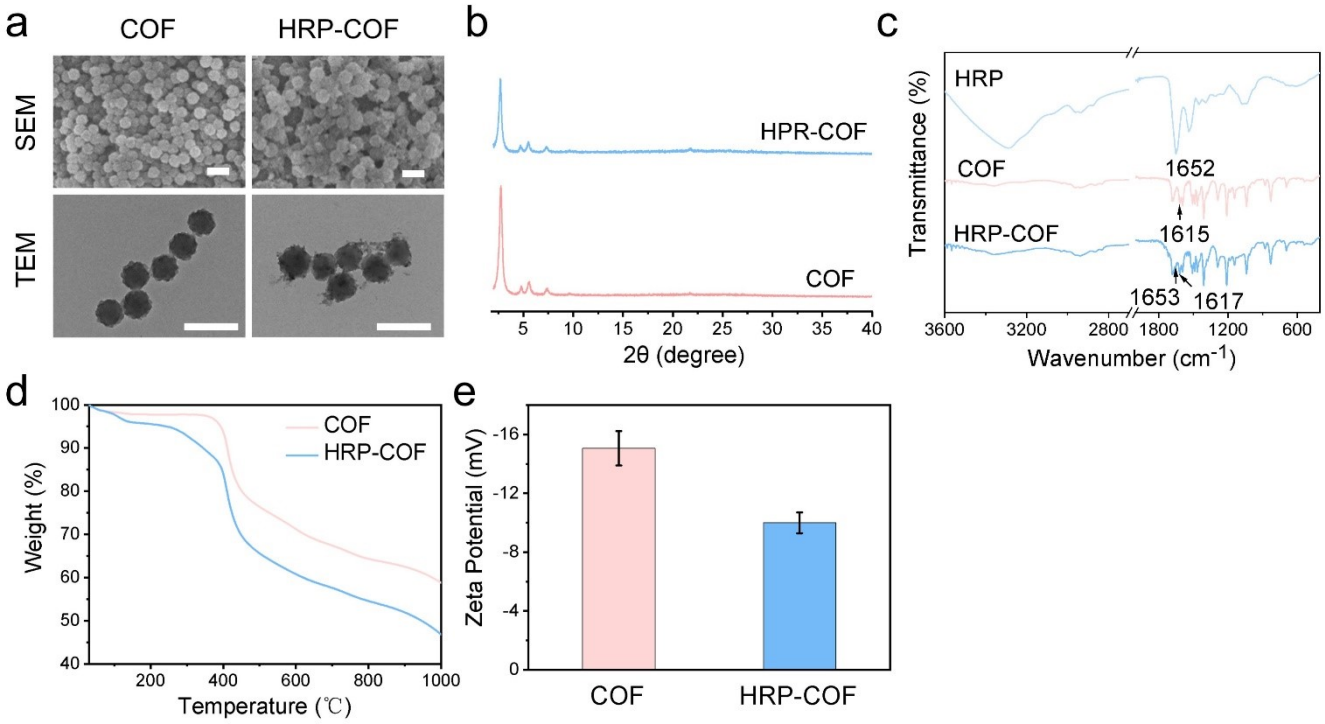

Fig. S11 Characterization of HRP-COF. (a) SEM and TEM images of the COF and the HRP-COF nanoparticles. Scale bars, 500 nm. (b) PXRD patterns of COF and the HRP-COF nanoparticles. (c) FTIR spectra of pure COF crystal, HRP and HRP-COF composite. (d) TGA curves of COF and HRP-COF composite in air. (e) Zeta potentials of the COF and HRP-COF nanoparticles (NPs). The error bar is the standard deviation from the mean (n = 3).

Supplementary note 4: Discussion for Fig. S12-S14

No obvious leaching of GOx from the GOx@COF was detected by measuring the enzyme concentration in the supernatant using the fluorescence assay (Fig. S12, ESI†). TEM images (Fig. S13, ESI†) confirmed that HRP@COF maintained its morphology over 24 hours in PBS (pH = 5.0, 6.0, 7.4). CLSM confirmed that the RhB-labeled HRP are evenly distributed within the COF (Fig. S14, ESI†).

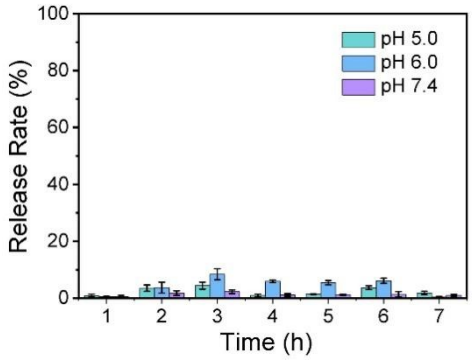

Fig. S12 Leaching of GOx from FITC-GOx@COF observed over 7 hours under various pH values. Leaching was assessed by calculating the release rate (%) based on the supernatant fluorescence intensity relative to the total fluorescence of loaded FITC-GOx.

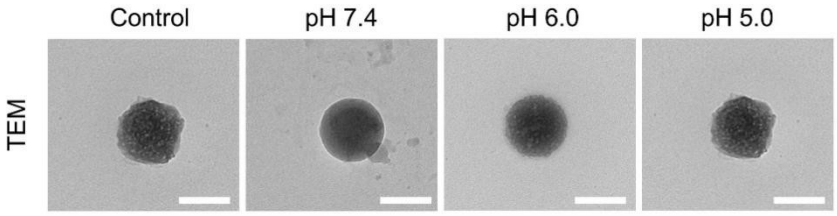

Fig. S13 TEM images of HRP@COF in PBS solution (pH = 5.0, 6.0, 7.4, 10 mM) at 25°C for 24 h. Scale bar, 100 nm.

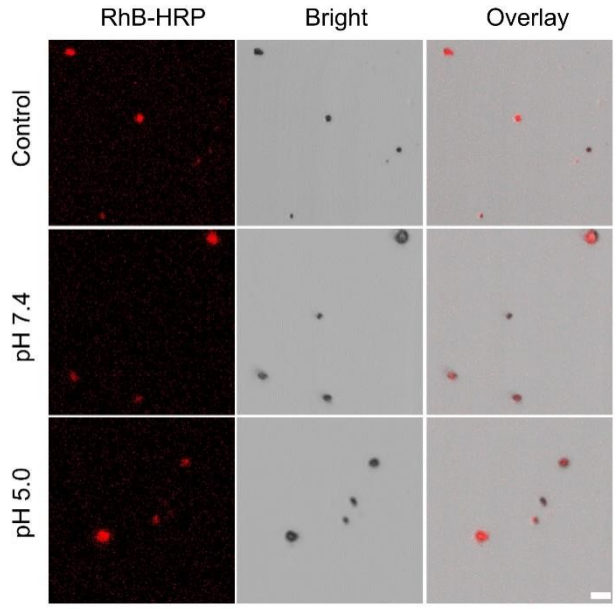

Fig. S14 Confocal microscopy images of the HRP@COF composite dispersed in PBS solutions with different pH values after 24 h, HRP was labeled with RhB (red). Scale bar, 200 nm.

Supplementary note 5: Discussion for Fig. S15

GOx could oxidize glucose producing gluconic acid and H_2O_2 accompanying with decrease in pH and O_2 amount. First, we monitored pH changes using a pH meter to assess the catalytic efficiency of GOx. Compared with COF solution, an obvious pH value drop was observed with the generation of gluconic acid in GOx&HRP@COF solutions (from 7.4 to 4.4) (Fig. S15a, ESI†). The other product of glucose oxidation, H_2O_2, was also detected using a commercial H_2O_2 kit. Similarly, GOx-catalytic H_2O_2 production is higher in GOx&HRP@COF solutions compared to that in COF groups (Fig. S15b, ESI†). Secondly，activity of encapsulated HRP was tested by oxidizing TMB in the presence of H_2O_2 with a blue product. When H_2O_2 and TMB were introduced into the GOx&HRP@COF solution, an evident colour changes from colorless to blue was observed with strong absorption at 652 nm in a concentration-dependent manner (Fig. S15c, ESI†), indicating the good catalytic ability of HRP encapsulated in GOx&HRP@COF solution.

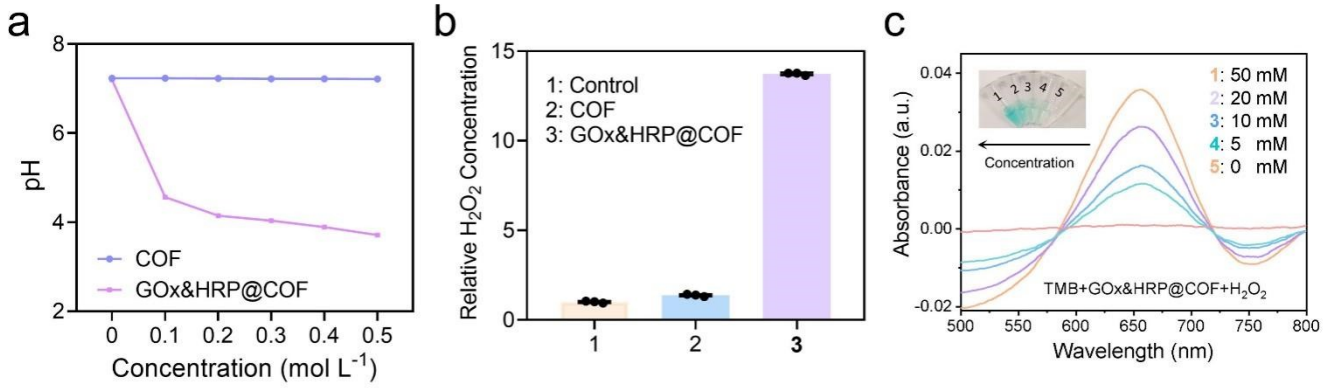

Fig. S15 Catalytic properties of GOx and HRP within GOx&HRP@COF. (a) The pH values of the COF and GOx&HRP@COF solution were treated with different concentrations of glucose solution. (b) Relative H_2O_2 concentration in solution after reaction of COF and GOx&HRP@COF with glucose, respectively. The error bar is the standard deviation from the mean (n = 3). (c) UV − vis absorbance and color changes of TMB oxidation of GOx&HRP@COF solution with different concentrations of H_2O_2 solution.

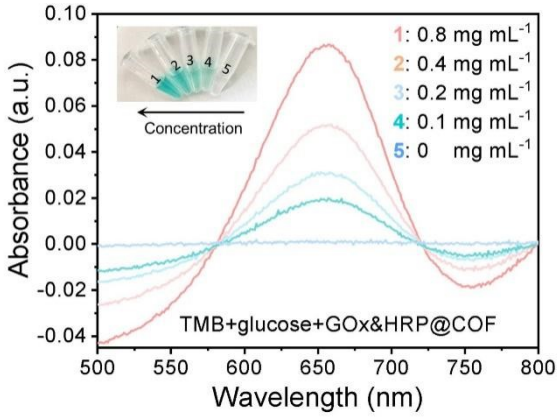

Fig. S16 UV − vis absorbance spectrum and visual color changes of TMB oxidation of GOx&HRP@COF solution with different concentrations.

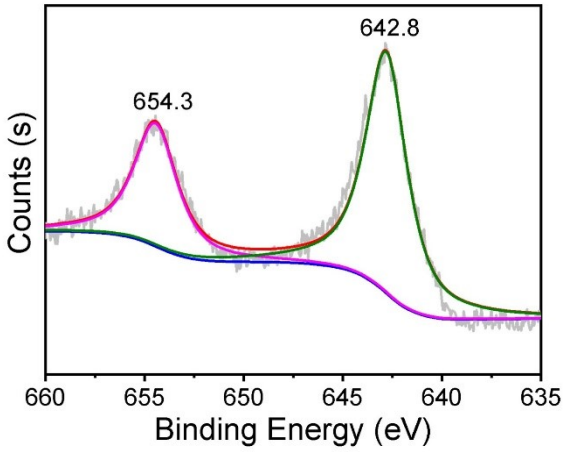

Fig. S17 XPS spectrum of Mn 2p in GOx&HRP@COF@MnO_2.

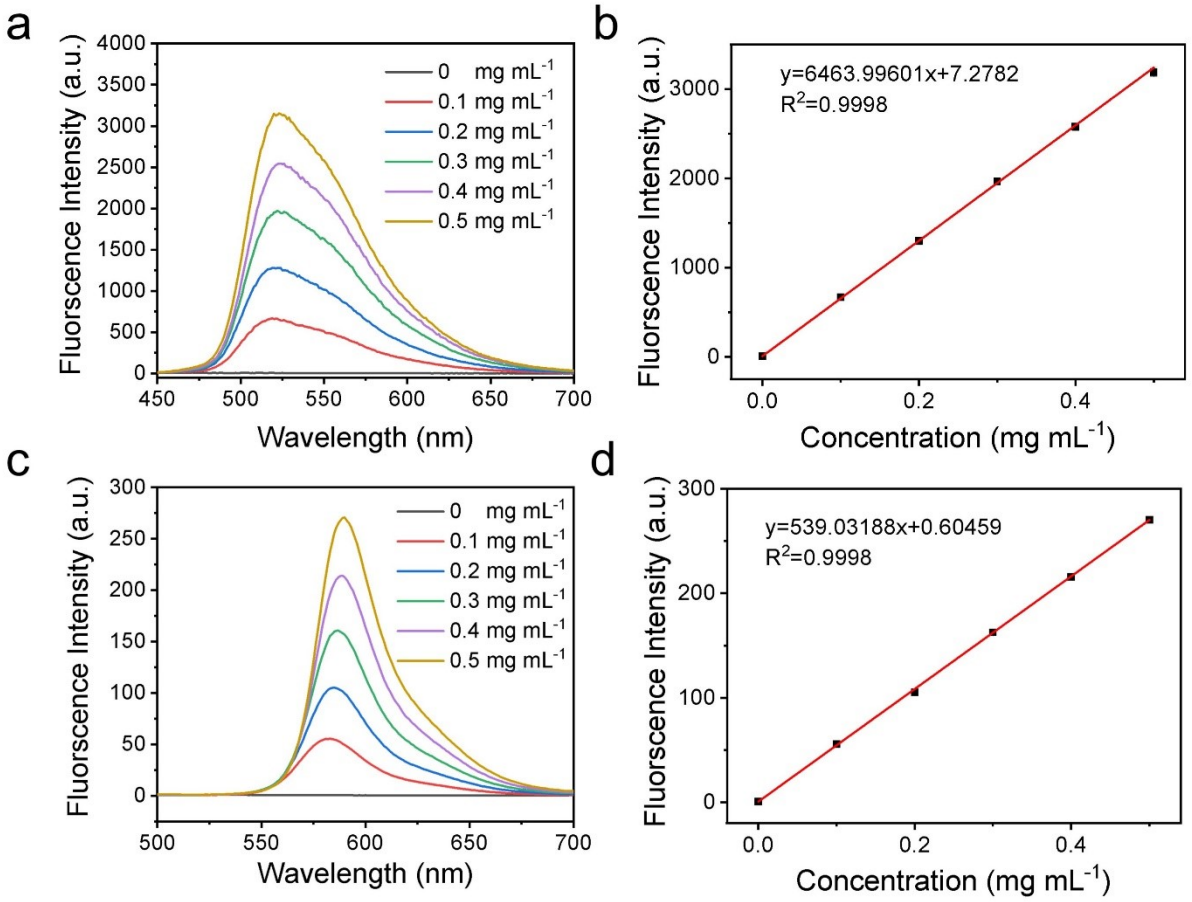

Fig. S18 Standard curve of FITC-GOx and RhB-HRP. (a) Fluorescence spectra of FITC-GOx with different concentrations. (b) Linear relationships between the fluorescence intensity of FITC-GOx at 525 nm and the FITC-GOx concentration. (c) Fluorescence spectra of RhB-HRP with different concentrations. (d) Linear relationships between the fluorescence intensity of RhB-HRP at 588 nm and the RhB-HRP concentration. The error bar is the standard deviation from the mean (n = 3).

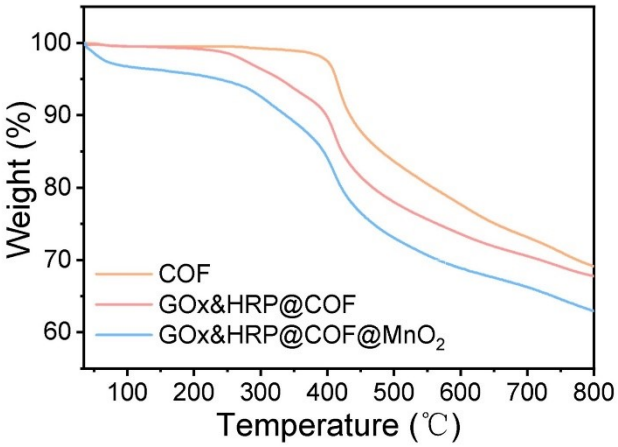

Fig. S19 TGA traces of COF, GOx&HRP@COF, and GOx&HRP@COF@MnO_2.

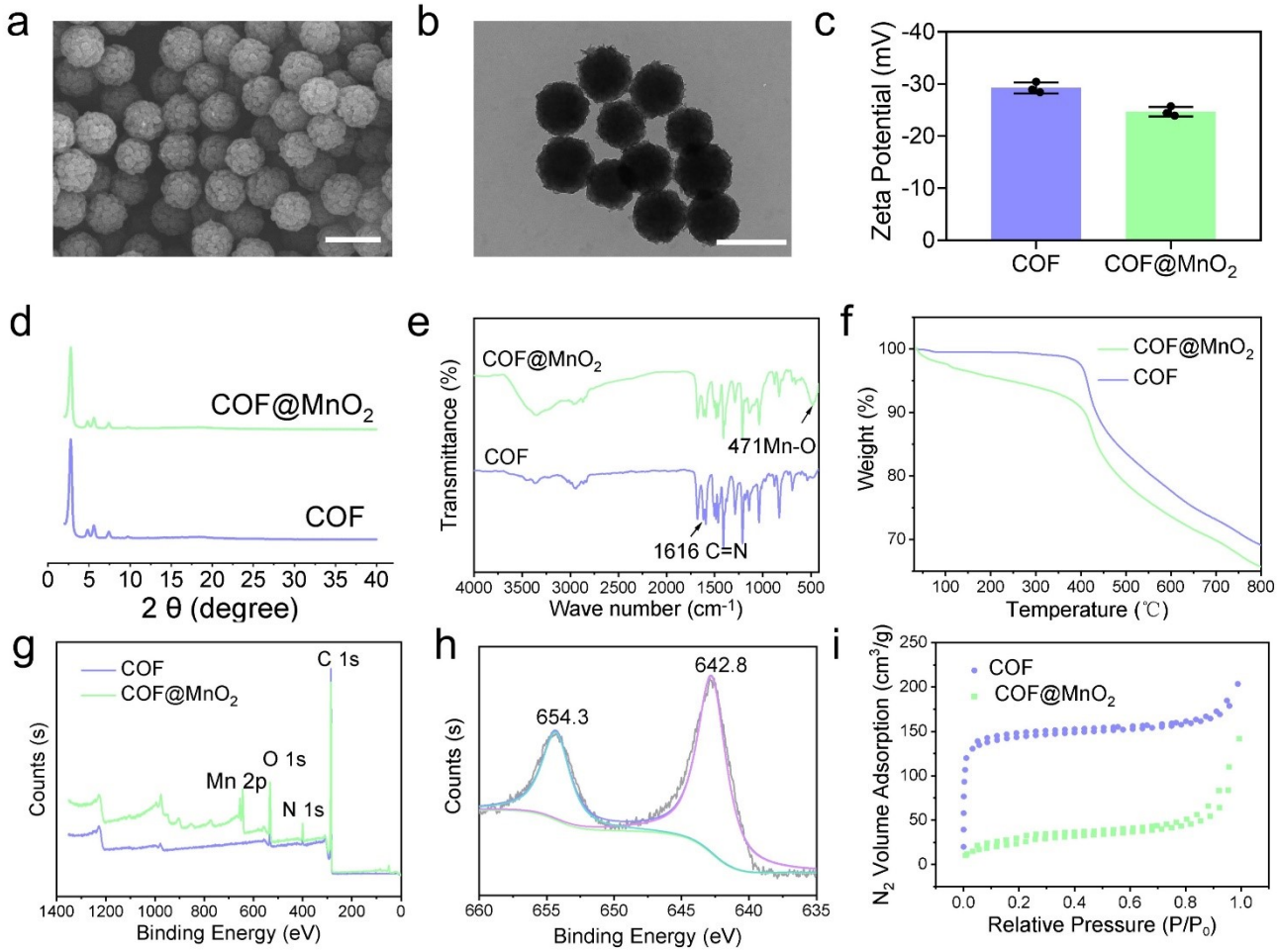

Fig. S20 Characterization of COF, COF@MnO_2. (a) SEM images and (b) TEM images of COF@MnO_2, Scale bar, 500 nm. (c) zeta potential value, (d) PXRD patterns, (e) FT-IR spectra, (f) TGA curves, (g) XPS spectra of COF and COF@MnO_2. (h) XPS spectrum of Mn 2p in COF@MnO_2. (i) N_2 adsorption and desorption isotherms at 77 K of COF and COF@MnO_2.

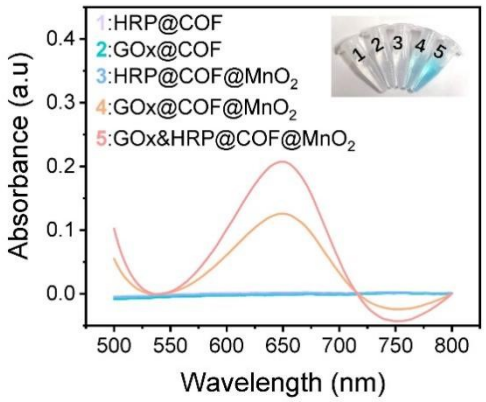

Fig. S21 UV − vis absorbance spectrum and visual color changes of TMB oxidation with different treatments.

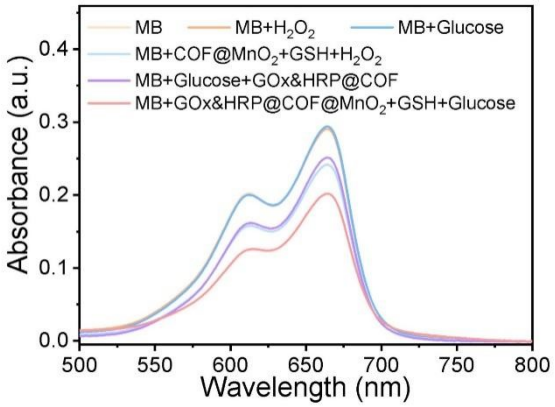

Fig. S22 UV − vis absorption spectra of MB treated with different treatments.

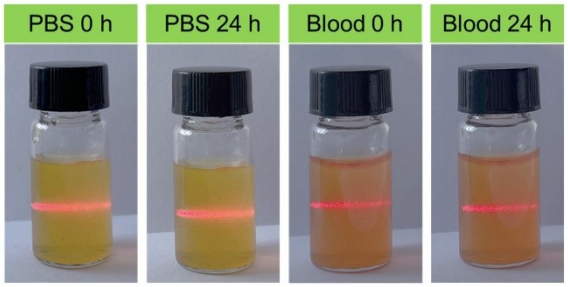

Fig. S23 Digital photographs of GOx&HRP@COF@MnO_2 in PBS and blood for 24 h. The observed Tyndall effect indicated that the PBS and blood dispersions of GOx&HRP@COF@MnO_2 are stable at least for 24 h.

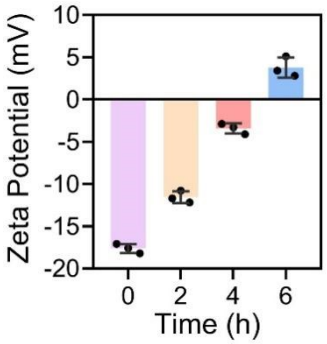

Fig. S24 The change of the zeta potential of GOx&HRP@COF@MnO_2 over time in the presence of GSH.

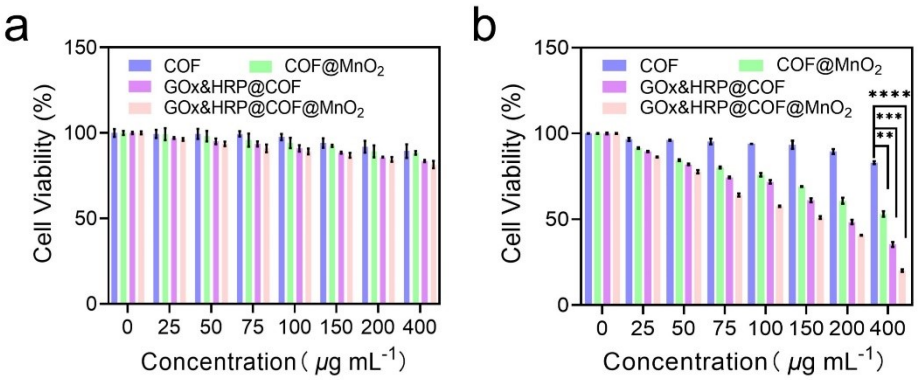

Fig. S25 Cell viabilities of (a) HL-7702 and (b) 4T1 cells after treated with various concentrations of COF, COF@MnO_2, GOx&HRP@COF and GOx&HRP@COF@MnO_2 (0, 25, 50, 75, 100, 150, 200, 400 μg mL^{-1}). The error bar is the standard deviation from the mean (n = 3). **p <0.01, ***p <0.001, ****p <0.0001.

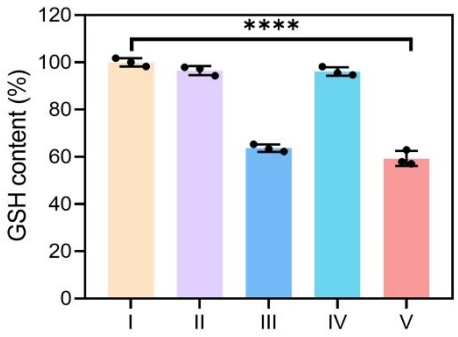

Fig. S26 Intracellular GSH depletion with different materials. The error bar is the standard deviation from the mean (n = 3). I: PBS; II: COF; III: COF@MnO_2; IV: GOx&HRP@COF; V: GOx&HRP@COF@MnO_2. ****p <0.0001.

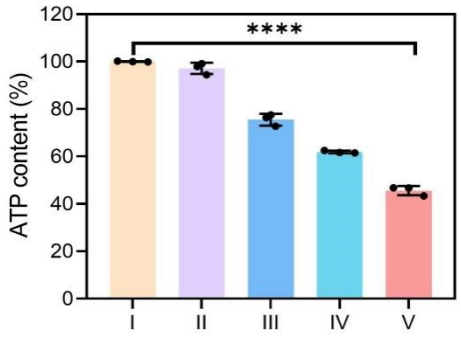

Fig. S27 Intracellular ATP depletion with different materials. The error bar is the standard deviation from the mean (n = 3). I: PBS; II: COF; III: COF@MnO_2; IV: GOx&HRP@COF; V: GOx&HRP@COF@MnO_2. ****p <0.0001.

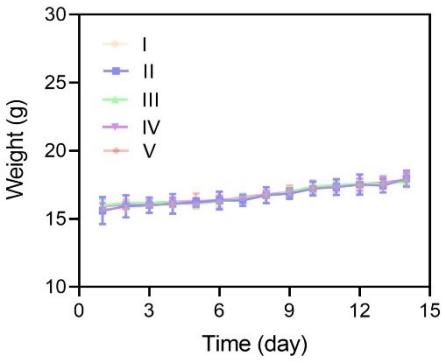

Fig. S28 Body weights of mice in the different groups. The error bar is the standard deviation from the mean (n = 5). I: PBS; II: COF; III: COF@MnO_2; IV: GOx&HRP@COF; V: GOx&HRP@COF@MnO_2. The error bar is the standard deviation from the mean (n = 5).

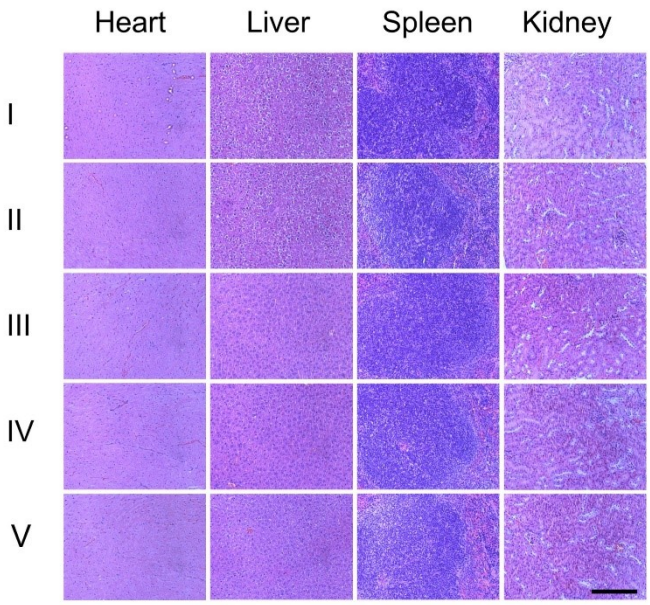

Fig. S29 Sections of major organs stained with H&E for the different groups, Scale bar, 100 μm. I: PBS; II: COF; III: COF@MnO_2; IV: GOx&HRP@COF; V: GOx&HRP@COF@MnO_2.

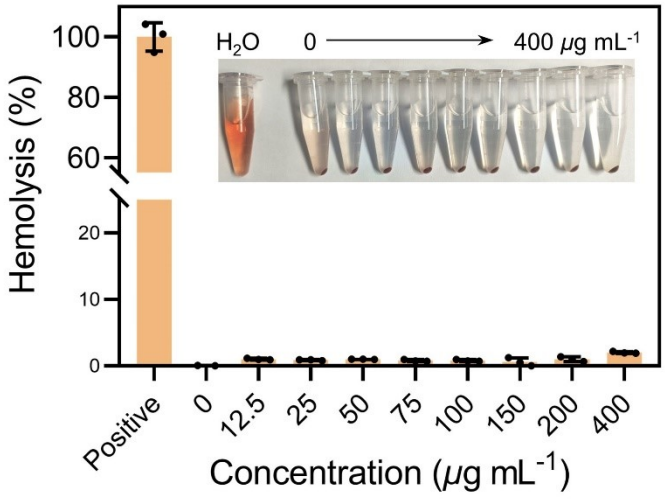

Fig. S30 Hemolysis measurement of GOx&HRP@COF@MnO_2 with various concentrations. PBS and ultrapure water were separately used as the negative and positive control, respectively. The error bar is the standard deviation from the mean (n = 3).

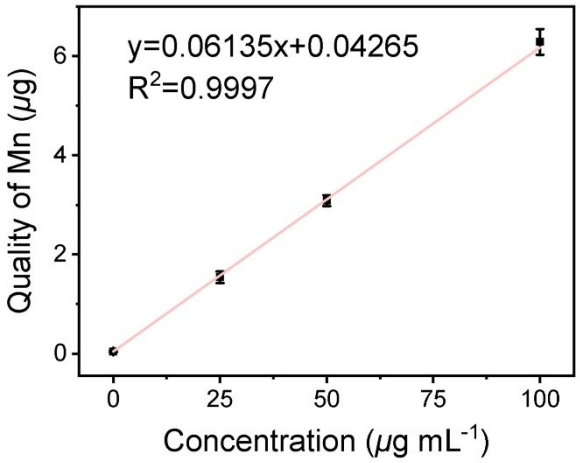

Fig. S31 Quantitative analysis the content of Mn in GOx&HRP@COF@MnO_2 with different concentrations by ICP-MS.

References

1. J. Feng, W.-X. Ren, F. Kong, C. Zhang and Y.-B. Dong, Nanoscale Covalent Organic Framework for the Low-Temperature Treatment of Tumor Growth and Lung Metastasis, *Sci. China Mater.*, 2022, **65**, 1122–1133.
2. S. Zhang, Y. Zheng, H. An, B. Aguila, C.-X. Yang, Y. Dong, W. Xie, P. Cheng, Z. Zhang, Y. Chen and S. Ma, Covalent Organic Frameworks with Chirality Enriched by Biomolecules for Efficient Chiral Separation, *Angew. Chem. Int. Ed.*, 2018, **57**, 16754-16759.
3. X. Wu, J. Ge, C. Yang, M. Hou and Z. Liu, Facile Synthesis of Multiple Enzyme-Containing Metal–Organic Frameworks in a Biomolecule-Friendly Environment, *Chem. Commun.*, 2015, **51**, 13408-13411.
4. J. Hu, F. Wang, F. Liu, W. Sun, Q. Jiang, Y. Liu, Y. Zhao and X. Liu, Effective Nanotherapeutic Approach for Metastatic Breast Cancer Treatment by Supplemental Oxygenation and Imaging-Guided Phototherapy, *Nano Res.,* 2020, **13**, 1111–1121.
5. K. Liang, R. Ricco, C. M. Doherty, M. J. Styles, S. Bell, N. Kirby, S. Mudie, D. Haylock, A. J. Hill, C. J. Doonan and P. Falcaro, Biomimetic Mineralization of Metal-Organic Frameworks as Protective Coatings for Biomacromolecules. *Nat. Commun.*, 2015, **6**, 7240.
6. P. Gao, M. Wang, Y. Chen, W. Pan, P. Zhou, X. Wan, N. Li and B. Tang, A COF-Based Nanoplatform for Highly Efficient Cancer Diagnosis, Photodynamic Therapy and Prognosis, *Chem. Sci.*, 2020, **11**, 6882-6888.
7. L. Cai, C. Hu, S. Liu, Y. Zhou, M. Pang and J. Lin, A Covalent Organic Framework-Based Multifunctional Therapeutic Platform for Enhanced Photodynamic Therapy via Catalytic Cascade Reactions, *Sci. China Mater,* 2021, **64**, 488–497.